IEEE Access
Multidisciplinary | Rapid Review | Open Access Journal

Received January 22, 2020, accepted February 7, 2020, date of publication February 12, 2020, date of current version February 26, 2020.

Digital Object Identifier 10.1109/ACCESS.2020.2973503

Monitoring in Near-Real Time for Amateur UAVs Using the AIS

NICOLÁS MOLINA-PADRÓN[1], FRANCISCO CABRERA-ALMEIDA[1], (Member, IEEE), VÍCTOR ARAÑA[1], (Member, IEEE), MILUŠE TICHAVSKA[2], AND BLAS-PABLO DORTA-NARANJO[1]

[1]IDeTIC, University of Las Palmas de Gran Canaria, 35017 Las Palmas, Spain
[2]Exmile Solutions Limited, London N21 3NA, U.K.

Corresponding author: Nicolás Molina-Padrón (nicolas.molina@ulpgc.es)

This work was supported in part by the Spanish Government Project under Grant TEC2017-88242-C3-3-R, and in part by the University of Las Palmas de Gran Canaria Project under Grant ULPGC2015-01. The work of Nicolás Molina-Padrón was supported by the predoctoral fellowship by the Agencia Canaria de Investigación, Innovación y Sociedad de la Información, through the "Canarias avanza con Europa" Program, co-funded by the European Social Fund.

ABSTRACT The use of drones or UAVs (unmanned aerial vehicles) for commercial or leisure purposes is increasingly common in our society. However, UAVs can also be used for other purposes that may compromise the privacy and safety of the population. For this reason, it has become necessary to enable the monitoring and identification of UAVs through a radio system with a license to avoid unwanted interferences. This article proposes the AIS (Automatic Identification System) as an alternative to monitor drone activities in near-real time. To do this, a prototype has been designed and integrated in an amateur UAV unit, enabling the transmission of UAV parameters through this system. AIS density testing has been carried out in selected zones of Gran Canaria (Spain), demonstrating the compatibility between the canonical usage of the AIS for vessels and its new proposed purpose for amateur UAVs.

INDEX TERMS Prototype, remote monitoring, UAV (unmanned aerial vehicles), radio navigation, AIS (automatic identification system), near-real time.

I. INTRODUCTION

In the last decade, the use of drones or UAVs (unmanned aerial vehicles) has increased significantly in many applications for different purposes. Such aircraft, which could have different dimensions and shapes, are capable of executing many tasks autonomously without onboard human control. Due to the use of these devices in some professional fields beyond the military field for which they were conceived, important challenges and improvements have been taken in fields such as agricultural harvesting, aerial imaging and transport of light goods [1]–[3]. Additionally, small drones, also called amateur drones (ADrs), are also used for recreational purposes by users of all ages, but they can also be used for illegal or terrorist purposes.

The extensive use of these flight units has involved important technological evolution, but it has also posed new security and privacy challenges for governments, companies and individual users [4], [5]. Social mistrust about the malicious usage of drones and the need to reduce risks in private zones have resulted in the development of international regulations for UAVs, which is still in progress [6]. For this reason, the main technological challenge to comply with UAV regulations and alleviate social mistrust with security and privacy measures consist of the development of amateur drone surveillance systems. ADr surveillance systems must be accurate and operate in real time, and these systems must support authorities to avoid voluntary or involuntary ADr intrusion in prohibited areas.

In the literature, different methods that can be used as amateur drone surveillance systems have been proposed [7], [8]. Such methods are strongly dependent on the nature of technology, but in all cases, the stages that must be complied by these surveillance systems are *detection* (the presence of a UAV must be detected early), *localization* (the location of the UAV must be known in terms of its latitude, longitude and elevation), *tracking* (the localization's evolution must be known at all times) and *control* (countermeasures must be performed to avoid the presence of UAVs in restricted airspace) [9]. Taking into account these stages, the current technologies available for UAV surveillance systems could be classified as *acoustic* (based on the acoustic signals generated by the

The associate editor coordinating the review of this manuscript and approving it for publication was Maurizio Magarini.

UAV engines), *optical* (UAV images are detected through cameras or similar devices, and then, the UAVs are located using 3D algorithms), *radar* (the UAV is considered the target and is detected by transmitted high-frequency pulses) and *radio frequency* (the UAV produces radioelectric emissions to communicate with a ground station, and these signals are detected and processed) [10].

With regard to acoustic technology, drone detection is based on recordings of the sounds produced by UAV engines or wings, and then, the acoustic signal is processed to locate and track the UAV using machine-learning techniques [11], [12] or other methods based on traditional statistical principles [13]. Generally, optical technology applied for drone surveillance uses visible or thermal image acquisition to detect the presence of drones, and then, 3D algorithms are applied to locate and track them [14], [15]. Radar technology scans the airspace continuously to detect drones, and then, radar signal processing is applied to distinguish between drones and other targets, such as birds [16], [17]. Finally, RF technology uses radioelectric emissions that are generated by drones as telemetry data to locate and track them [18], [19]. Moreover, there exist many commercial solutions based on RF technology. Usually, amateur UAVs use paired transceivers to control and monitor their activities on the 433 MHz band, sharing a common coding between the flight unit and the base station [20]. In this solution, only one UAV can be monitored by a base station, so it is not possible to cover an area where multiple drones are flying. However, commercial devices that comply with this purpose exist. One of them is DJI AeroScope, a centralized system that can detect and process UAV communications in the 2.5/5.8 GHz bands and extract information every 2 seconds, with a maximum range of 50 km under ideal conditions [21]. However, this solution is based on DJI drone models, so it was not developed for all UAV protocols. Another commercial system is the CRFS drone detector [22], which uses spectrum monitoring techniques to detect the presence of drones through telemetry emissions; however, this system cannot be used to identify them.

Regarding acoustic and optical technologies, the short detection range is the main limitation to amateur drone detection. In addition, radar technology is limited by the high cost and societal rejection of a massive deployment of radar networks in cities. For these reasons, RF technology is one of the most studied solutions to develop amateur drone surveillance systems.

The above amateur drone surveillance systems do not depend on any type of data or parameters that have been transmitted voluntarily by drones. Therefore, a new classification system is necessary to study those drone surveillance systems: *known-monitoring methods* (UAV operators voluntarily send the UAV positions to be detected through RF emissions) and *unknown-monitoring methods* (operators do not want the UAV to be detected by RF emissions). On the one hand, unknown-monitoring methods are the key to resolving security breaches because, in most cases, a drone entering a prohibited zone does not want to be detected. On the other hand, known-monitoring methods are specifically interesting for drone fleet control, but they are not useful in terms of security. A typical unknown-monitoring method based on RF technology consists of the integration of ADS-B (Automatic Dependent Surveillance – Broadcast) [23], [24], which is used to identify and monitor aircraft, on a UAV, allowing its detection and even the identification and monitoring of it. Although ADS-B is not a critical air navigation system, if it is used in drones, it would increase the number of vehicles that use this system in a given region and then worsen the chances of detecting these vehicles [25], where the aircraft transmitted signal could overlap and information would be lost.

In the maritime domain, the identification and monitoring of vessels is addressed through the AIS (Automatic Identification System). The AIS is a standardized communication system that allows a vessel to transmit static, dynamic and voyage parameters to other vessels, coastal stations and satellites. It presents great robustness in radioelectric propagation, even under harsh tropospheric conditions [26], giving rise to a coverage of more than 40 km - 60 km in the line-of-sight [27] of a single transceiver unit. Additionally, the messages are not encrypted, so any user with an AIS receiver can monitor the status of maritime traffic. Commonly, the AIS was conceived to support maritime rescues and avoid vessel collisions. When the Class B AIS was introduced in 2007 [28], the AIS was democratized and began to be used for different purposes in addition to maritime security. In the environmental field, the AIS can be used as a weather station for maritime devices [29] or to estimate the potential effects of tsunamis [30], and it is an important information source for estimating pollution by vessels [31], [32]. In vehicular networks, the AIS has been implemented in aerial drones [33] and unmanned maritime vehicles [34] for different research tasks. Finally, the AIS will evolve into a new standardization in the coming years, called the VDES (VHF Data Exchange System). The VDES will increase the number of channels and other aspects that could help introduce new uses and applications [35].

In this article, we describe the development of a prototype integrated into an amateur drone that enables, through an AIS transceiver, the identification and monitoring of this device in near-real time. Section I presents the problem to be solved and the most relevant technical details about the AIS and the MAVLink protocol. Section II details the design and integration of the prototype, which is not optimized in terms of power consumption. In Section III, the algorithm implemented for the correct operation of the prototype is presented. Section IV describes the tests performed with the prototype in a real-world environment; finally, Section V outlines the conclusions reached with this work.

A. AIS (AUTOMATIC IDENTIFICATION SYSTEM)

The AIS is a maritime communications system of mandatory use for certain types of vessels based on regulation by the IMO (International Maritime Organization) since 2003. This regulation is primarily applicable to vessels of large

dimensions and to passenger ships [36], [37]. Each vessel is associated with a unique identifier, called the MMSI (Maritime Mobile Service Identity), used by ships and other units, such as aircraft and buoys, and transmits static (name, MMSI, dimensions), dynamic (speed, position, heading) and voyage (origin and destination ports) information through a series of protocols while transmitting and receiving this same information to and from AIS-equipped vessels and AIS receiving stations in range.

This system operates in the maritime VHF band on two frequencies: AIS-1 (161.975 MHz) and AIS-2 (162.025 MHz), with a channelization of 25 kHz and a bit rate of 9,600 bps. It uses an NRZI (non-return-to-zero inverted) coding scheme and an FM-GMSK (frequency modulation - Gaussian minimum shift keying) modulation [38]. The main feature of the AIS is the access scheme to the TDMA (time division multiple access) medium, which allows each vessel to compete with the rest to transmit its information in a slot of 26.67 ms, with a low probability of collision among communications.

The AIS system can be classified into different categories depending on the application for which it is intended. The differences between these types of AIS systems lie in their TDMA scheme and maximum power transmitted. The main types are class A AIS, with an SOTDMA (self-organized time division multiple access) scheme and 12.5 W, and class B AIS, with a CSTDMA (carrier-sense time division multiple access) scheme and 2 W. Generally, class A AIS is integrated into ships that must include the AIS in their onboard systems, while class B AIS is usually optionally integrated into the rest of the vessels. In addition, there are other types of AIS, such as AtoN (Aid-to-Navigation) and SART (Search and Rescue Transponder), and AIS base stations for other specific purposes. As shown in Figure 1, the AIS data transmitted from ships and other devices are collected by the AIS receiver stations (AIS data acquisition network), which provide Internet access to distribute these data for different applications and services (AIS data distribution network).

The AIS includes a total of 27 message types. Among these messages, in relation to this work, it is important to underline message types 18 and 24, which represent the static and dynamic information of class B AIS, respectively. The use of each message depends on the type of AIS equipment, as well as the information transmitted and updated according to the AIS type and the speed of vessels, as indicated in Table 1.

TABLE 1. Report rates for class A/B AIS equipment.

Class A AIS	
Movement status	Report rate
Anchored or moored vessels	3 minutes
Sailing at 0 - 14 knots	10 seconds
Sailing at 14 - 23 knots	6 seconds
Sailing at 0 - 14 knots and changing course	3.33 seconds
Sailing at 14 - 23 knots and changing course	2 seconds
Sailing faster than 23 knots	2 seconds
Sailing faster than 23 knots and changing course	2 seconds
Class B AIS	
Less than 2 knots	3 minutes
Greater than (or equal to) 2 knots	30 seconds

1 knot is equal to 0.514 m/s

Finally, AIS uses the NMEA0183 protocol for the communication of messages between onboard naval electronics units [39]. This protocol, which is also used by GPS receivers,

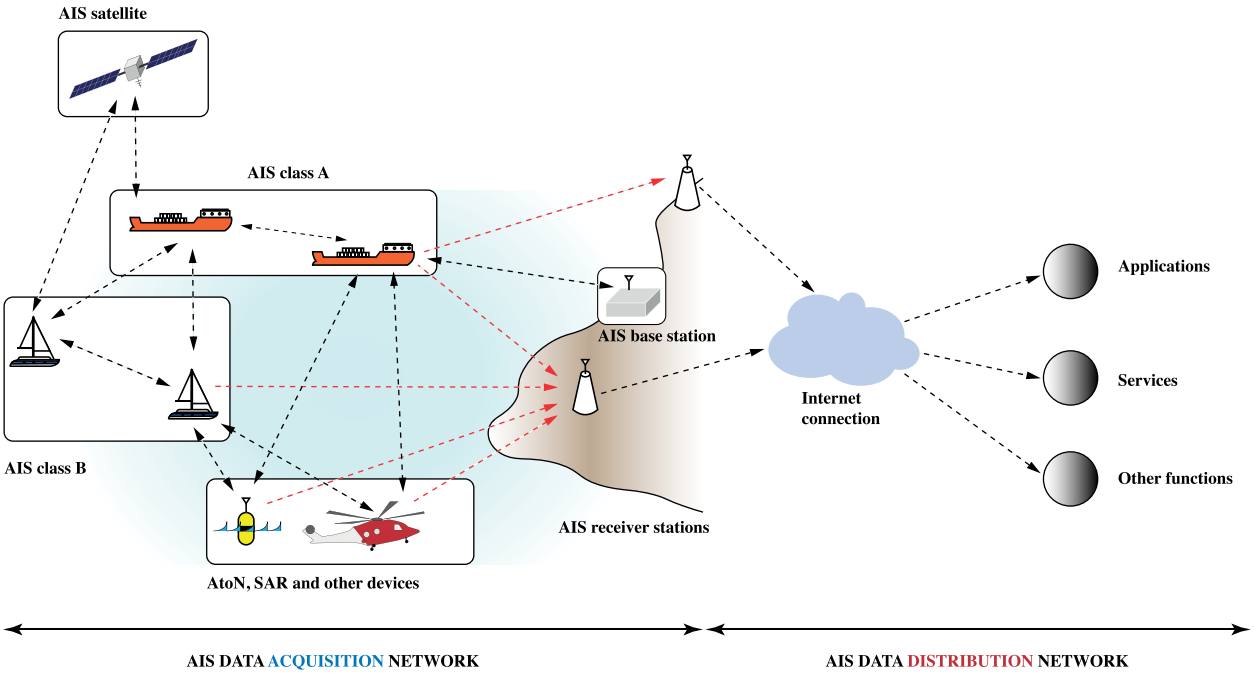

FIGURE 1. AIS data acquisition and distribution networks.

uses 6-bit ASCII data encoding with differential signals, and its format is as follows:

```
AXXYYY,DATA,*ZZ<0D><0A>
```

The digit A is the delimiter of the message, which can be ! or #. The digits XX represent the type of device that sends the message, YYY the type of data that contains the message, and DATA the payload of the message, and the character * ends the message. The digits ZZ represent the hexadecimal checksum of the message, and they are calculated by performing an exclusive OR operation on the previous consecutive digits, including commas. The command ends with the hexadecimal digits of the carriage return (0D) and line feed (0A).

B. MAVLINK PROTOCOL

The MAVLink protocol is a message library for monitoring the activity of UAVs and establishing a communication channel between the drone and a ground station [40], [41]. These libraries are free and available in both C and Python.

MAVLink works with different types of data, usually characters, floating and binary, and the size of the messages occupies a memory space between 8 and 263 bytes. The structure of a MAVLink frame is represented in Figure 2.

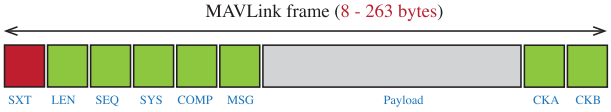

FIGURE 2. Structure of a MAVLink frame.

The SXT field indicates the beginning of the frame. LEN indicates the size of the payload. SEQ alerts about packet losses. SYS is the identifier of the UAV or ground station. COMP indicates the units connected to the UAV or the ground station. The payload includes all of the information that is to be transmitted, and the CKA and CKB values are the checksums associated with the sending of the frame.

The information contained in the MAVLink messages can be incredibly varied and includes everything from frames relating to GPS (position, heading, speed) to the values collected from the sensors integrated within the UAV (temperature, humidity, pressure).

II. PROTOTYPE ARCHITECTURE AND DESIGN

As shown in Figure 3, the prototype is formed by two parts: the *UAV platform*, which comprises the UAV support structure, a flight control module with a GPS antenna, a 433 MHz telemetry unit and a LiPo battery, and the *UAV payload*, which contains the following subsystems:

- *Control unit*, which includes a processor to collect UAV data and apply the appropriate format for communication as an AIS message.
- *Communication unit*, composed of a class B AIS transceiver to transmit the data received from the control unit.

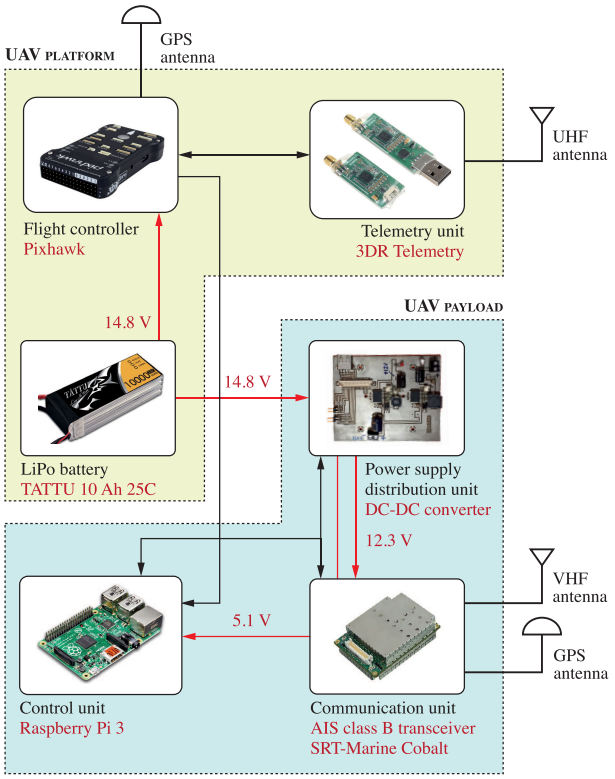

FIGURE 3. Block diagram of the prototype.

- *Power supply distribution unit*, consisting of a DC-DC converter, based on high efficiency converters, which allows generation of the necessary voltages, extracted from the LiPo battery, for the UAV and the integrated payload.

Only considering the UAV platform with a total weight of 988 g, the power consumption of the system is 238.2 W. This value has been obtained through a software simulation with the eCalc online tool [42], which shows a maximum flight time of 15 min. The payload has a weight of 268 g and a power consumption of 0.26 A, so it will reduce the maximum flight time to 13.1 min.

A. UAV PLATFORM

The amateur drone in which the prototype is integrated is the Y6 model produced by 3D Robotics [43]. It is a tricopter formed by three arms, with two rotors each, and three support legs. It has an integrated flight controller based on the Pixhawk model and a telemetry unit that operates at 433 MHz. Considering the UAV mechanical mounting, flight controller and LiPo battery, this platform has an approximate weight of 988 g, and its dimensions are shown in Figure 4.

The Pixhawk flight controller [44] operates under the APM firmware, loaded on a microSD card, and communicates with the drone's sensors and actuators. The main ports included are 2 serial, 2 USB, 1 SPI, 2 ADC, 1 I2C and 1 CAN, plus two telemetry ports, one GPS port, one power port and one output

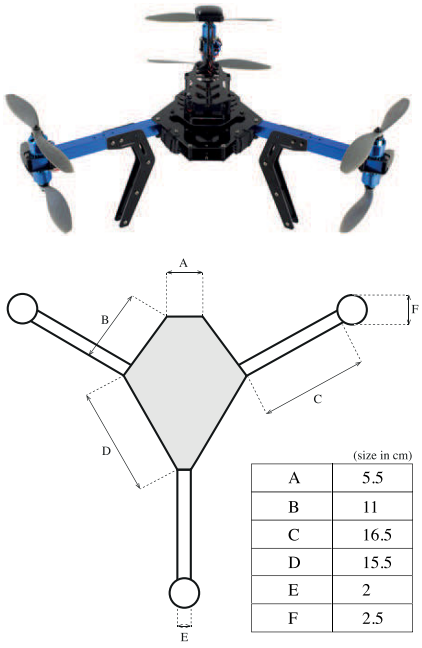

(size in cm)

A	5.5
B	11
C	16.5
D	15.5
E	2
F	2.5

FIGURE 4. Dimensions of the drone.

port to a buzzer. To connect to the payload, a USB connection is used to transmit the MAVLink telemetry frames.

In terms of power supply, a LiPo 4S1P battery with a 10,000 mAh capacity is used for feeding 14.8 V to all UAV subsystems, including the payload. The LiPo battery weighs 247 g.

B. CONTROL UNIT

A microcontroller based on a Raspberry Pi 3 model B circuit board is integrated into the payload [45]. The Raspberry Pi is a well-documented platform, and its usage is easy, allowing fast prototype development. Additionally, this platform has been used previously to implement AIS receivers [46], [47], but there are no commercial solutions for AIS transceivers in Raspberry Pi. This board includes a Broadcom BCM2837 processor, capable of running a Linux Debian operating system from a microSD card. This device consists of a GPIO interface to control the data inputs and outputs and includes both Ethernet and WiFi connections. Its configuration includes Python libraries to interpret the MAVLink commands it receives from the flight controller, in addition to the firmware developed for the prototype. In terms of power consumption, an increment of 0.774% over the UAV power consumption without payload and a weight contribution of 40 g are assumed for the microcontroller.

C. COMMUNICATION UNIT

A class B AIS transceiver based on the Cobalt module of SRT-Marine is used [48]. It is an SDR (software defined radio) unit that operates at AIS-1 (161.975 MHz) and AIS-2 (162.025 MHz) frequencies, with a sensitivity of −110 dBm, includes an integrated GPS unit and complies with the technical aspects included in ITU-R Recommendation M.1371-5 [49]. The prior configuration of this module was carried out using the proAIS2 software, which allows assigning a name and an MMSI to the device. The interfaces that make up the Cobalt module are classified as follows:

- *Serial and power interface*: through a Hirose DF13-40P-1.25V connector located on the front of the device, serial data can be transmitted and received via USB, SPI, NMEA0183 and NMEA2000. This same connector provides the device with the necessary pins for its feed.
- *RF interface*: using two Hirose U.FL-R-STM connectors, located at one of the sides of the module, this interface enables the use of VHF and GPS antennas.

One important aspect about this module is in relation to the transmission process. The Cobalt module will transmit the first AIS message as long as a GPS message has been previously received. Moreover, if the GPS signal is lost, the Cobalt module cannot transmit the AIS messages until the GPS signal has been recovered. In terms of power consumption, an increment of 0.535% over the UAV power consumption without payload and a weight contribution of 46 g are assumed for the AIS transceiver.

D. POWER SUPPLY DISTRIBUTION UNIT

To feed the components of the payload, a power distribution source based on high efficiency DC-DC converters (Switcher High Efficiency Regulators), able to accept voltages between 12.5 V and 18 V, has been developed. At its input, it receives 14.8 V from a LiPo 4S1P battery, and it outputs voltages of 5.1 V to power the Raspberry Pi and 12.3 V to feed the Cobalt AIS transceiver through a Hirose DF13-40P-1.25V connector. In terms of power consumption, an increment of 0.305% over the UAV power consumption without payload and a weight contribution of 46 g are assumed for the DC-DC converter.

E. PAYLOAD INTEGRATION

The connection scheme between payload modules and UAV platform elements is shown in Figure 5.

The Raspberry Pi 3 microcontroller is connected to the Pixhawk flight unit via a serial port through a USB-A to mini-USB male-to-male cable, allowing MAVLink messages from the UAV flight unit to be received and stored. The DC-DC converter is supplied with 14.8 V from the UAV LiPo battery. This voltage is distributed to the payload modules, where the AIS transceiver is supplied with 12.3 V and the microcontroller with 5.1 V. Additionally, this board facilitates the connection between the AIS transceiver and the microcontroller because it includes the pin routings of the Hirose DF13-40P and USB connectors, which are used by both modules. Through a Hirose DF13-40P cable, the DC-DC converter board is connected to an AIS transceiver, allowing AIS messages that will be processed by the microcontroller to be transmitted and received. A USB-A male-to-male cable is used to connect the microcontroller and DC-DC converter board.

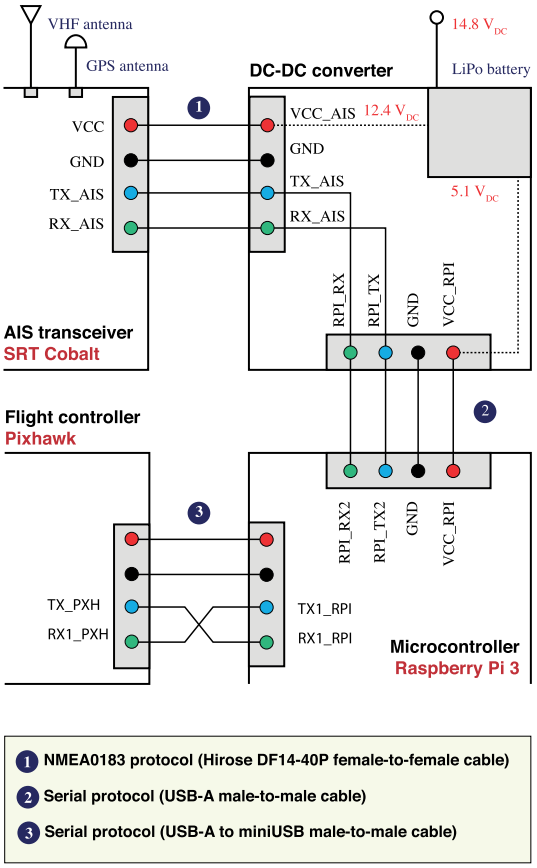

FIGURE 5. Payload module interconnection.

III. PROTOCOL FOR UAV MONITORING AND IDENTIFICATION

The procedure for generating AIS messages with the UAV's height is presented in Figure 6 and includes the following steps:

- *Step 1*. The UAV control firmware is implemented in the Pixhawk flight unit. Through MAVLink frames, the UAV obtains parameters from sensors, actuators and other integrated devices and then transmits them as telemetry messages. Among these telemetry messages, the UAV height is found.
- *Step 2*. The MAVLink frames are interpreted in the Raspberry Pi using the PyMAVLink libraries. These frames include the height parameter, which is extracted and converted as an NMEA0183 message. The UAV height is included in the HDT (heading true) field, presented in an AIS type 18 message, and is sent via a serial port from the Raspberry Pi to the AIS transceiver.
- *Step 3*. The AIS transceiver reads the NMEA0183 message, and it is processed as an AIS type 18 message.
- *Step 4*. Additionally, the date is extracted from the GPS unit integrated into the AIS transceiver. This information is added to and stored within the internal memory of the Raspberry Pi, thus providing an accurate date of when the AIS message was sent.

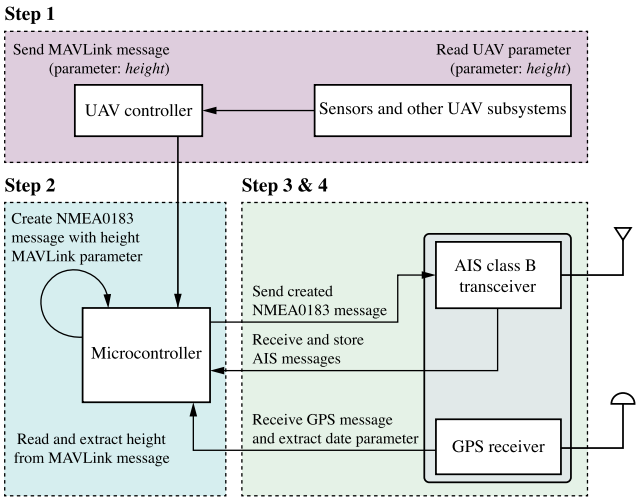

FIGURE 6. Procedure to acquire, generate and transmit an additional UAV parameter as an AIS message.

Algorithms 1 and 2 represent the pseudocodes of the processes implemented in the Raspberry Pi. Algorithm 1 starts loading the MAVLink libraries and extracts all the functions that allow the flight controller to be connected with external devices. The UAV height is extracted with the `get_height_mavlink` function. A variable is stored with the structure of the HEHDT message, where the UAV height is added without the message's checksum. To calculate the HEHDT message checksum, an XOR operation is gradually applied among consecutive characters from first ($) to last (∗), and the result is converted to hexadecimal format. The checksum is added as a hexadecimal character into the body of the initial HEHDT message. Then, it is sent via a serial port to the AIS transceiver and is stored in the internal memory of the Raspberry Pi with the AIS messages received.

Algorithm 1 AIS Message Generation With UAV Information

```
load MAVLINK_LIBRARY
loop
  uav_param ← get_height_mavlink(height)
  init_message ← "$HEHDT," + uav_param + ",T*"
  init k = 0
  for k to max(init_message)
    checksum ← checksum ⊕ init_message(k)
    if k == max(init_message)
      checksum ← convert_to_hexadecimal(checksum)
    end if
  end for
  end_message ← init_message + checksum
  send_serial(end_message)
  store_message(end_message)
end loop
```

Algorithm 2 assigns the UTC (Universal Time Coordinated) time when the event occurred to each transmitted or received AIS message. When a GPS GGA (Global Positioning System Fix Data) message is received, the UTC

Algorithm 2 AIS Message Storage With Datetime Information

```
loop
  gps_message ← gps_message_receive()
  if ais_message_receive() or ais_message_transmit()
    gps_message ← decode(gps_message_gga)
    date_time ← extract_datetime(gps_message)
    store_message(ais_message, date)
  end if
end loop
```

time of the position is extracted from its parameters. If an AIS message has been transmitted or received, then the UTC time of the last GPS message received is added to the AIS message. Thus, a list of transmitted and received AIS messages with the appropriate UTC time is stored.

IV. TEST AND MEASUREMENT

First, we proceed with a test of the AIS channel density index by using data provided by MarineTraffic and measurements made with the prototype in different environments of Gran Canaria (Spain). Second, a scheduled UAV flight is launched to verify the capability of the prototype in terms of identification and monitoring of its trajectory.

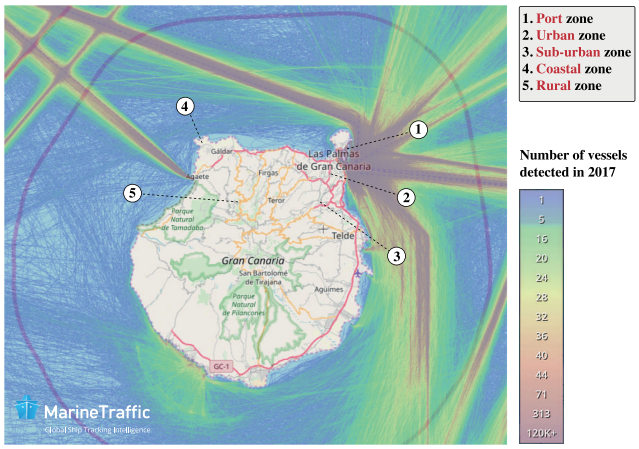

FIGURE 7. Testing areas represented in a map of Gran Canaria, Spain (AIS-based vessel traffic density map extracted and modified from the MarineTraffic website, https://www.marinetraffic.com/).

TABLE 2. MarineTraffic top 5 receiving stations based on class A received positions (messages) per minute.

Country	Station location	Station ID	Last signal (UTC)	Class A messages
	De Wacht	2676	2018-11-14 11:39:00	3016.9
	Rotterdam	2593	2018-11-14 11:39:00	2186.6
	Rotterdam	591	2018-11-14 11:39:00	2047.9
	Rozenburg	3283	2018-11-14 11:39:00	1748.9
	Eggesbones	1045	2018-11-14 11:39:00	1663.2

A. AIS CHANNEL DENSITY

The MarineTraffic Network [50], for instance, is characterized by over 3,729 proprietary cross-continentally installed nodes. Table 2 shows the top 5 according to the number of class A messages received per minute. In this table, it can be seen that De Wacht (The Netherlands) Station_ID node 2676 receives an average of 3069.1 messages per minute.

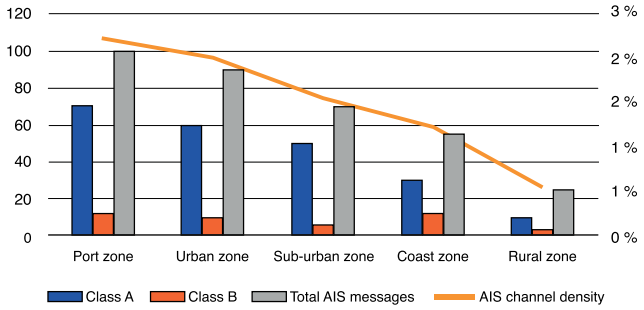

FIGURE 8. UAV messages received through the AIS in different environments of Gran Canaria.

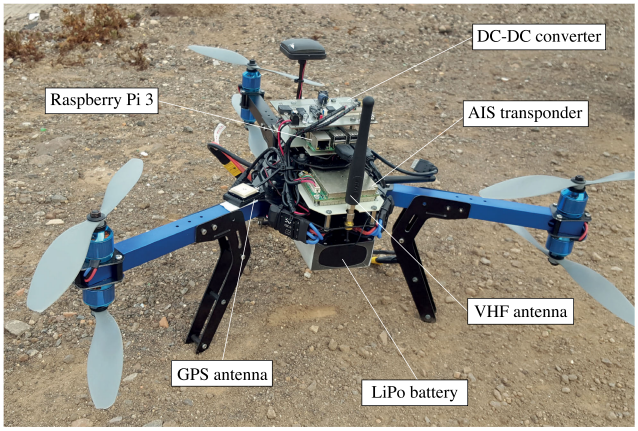

(a) Prototype mounted on the UAV platform

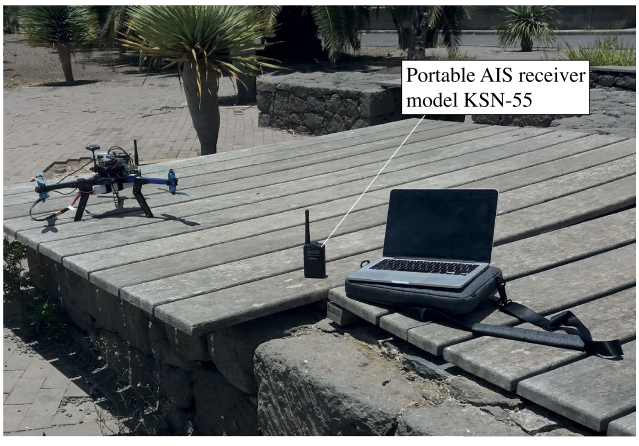

(b) Portable AIS receiver KSN-55

FIGURE 9. Prototype mounted on the UAV platform and AIS receiver KSN-55.

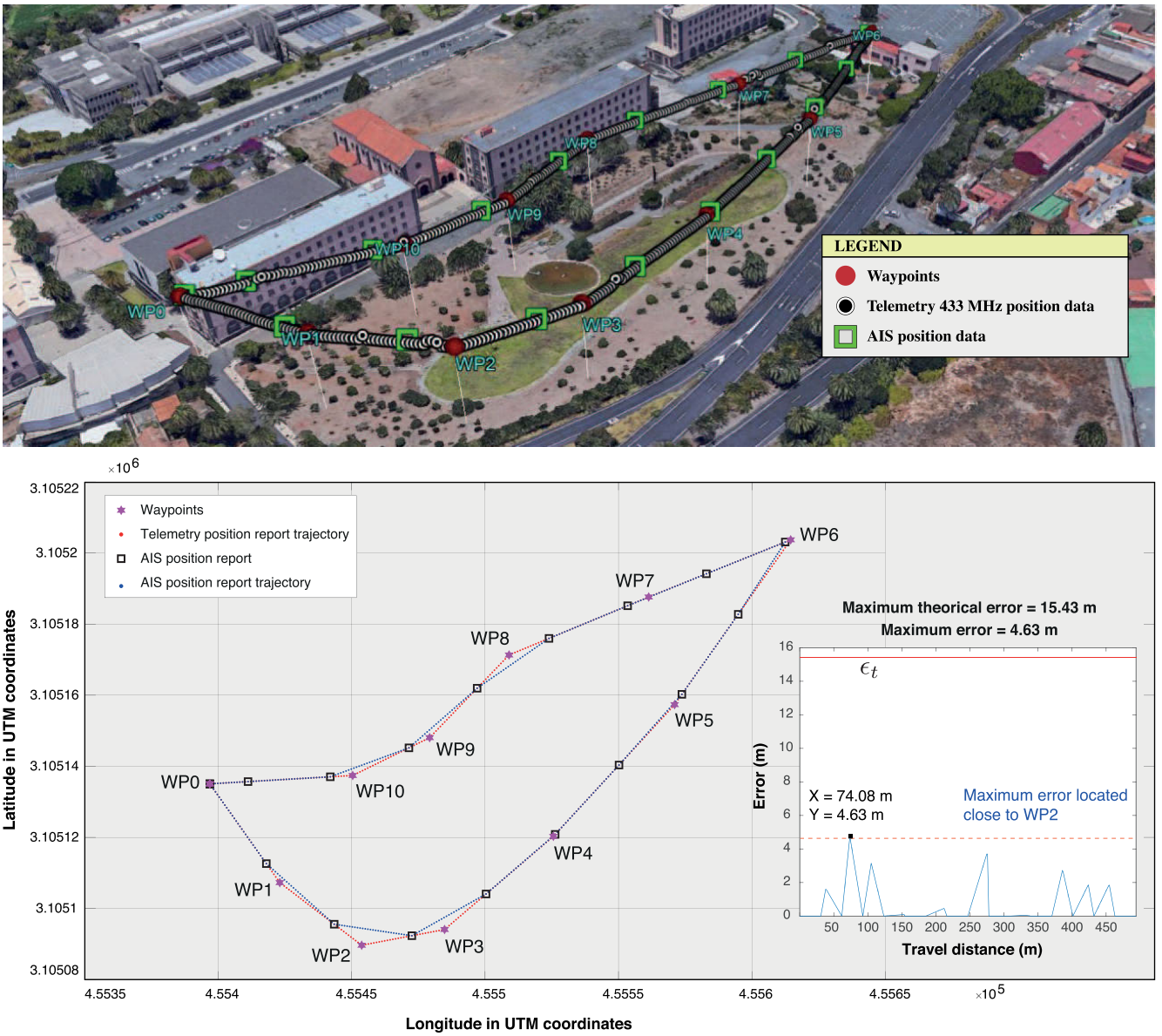

FIGURE 10. Tridimensional and bidimensional representations of the trajectories generated by AIS and 433 MHz telemetry data, and error between both trajectories.

Since the maximum number of messages is 4,500 [51], the density of the channel is 68.2% in this node. Other nodes, such as those at Rotterdam (The Netherlands), Rozenburg (The Netherlands) and Eggesbones (Norway), have indexes below 50%.

However, 97.3% of MarineTraffic nodes (3,627 nodes) operate with densities below 10%. This corresponds to fewer than 450 messages per minute. This value is low enough to conceive of the idea of potential usage of these channels for the monitoring of other vehicles, such as UAVs.

On the island of Gran Canaria (Spain), the MarineTraffic Network has several installed nodes. Among them is BMT-IDETIC Station_ID 1609, located in the ULPGC Science and Technology Park [52]. This station receives approximately 362 messages per minute (density of 8%). Other receiving stations located on the island receive a similar number of messages.

To verify the proper use of the AIS system in a UAV, we have configured the UAV in loiter mode, which allows it to be fixed in a certain position and at a height of 20 m above the ground. The AIS channel is thus measured in these conditions. With the stored data, we decode the information and construct a histogram, classifying the messages according to their class. The mentioned test has been carried out in different environments, which are represented in Figure 7 in terms of annual vessel density in Gran Canaria.

Figure 8 shows the average messages of each class and the total per minute received in each environment. In addition, the occupation density of the AIS channel is shown. In these measurements, it is observed, as in all zones, that the number

of messages received is quite low such that the occupation density of the channel exhibits values of approximately 1–4.5%. The AIS channel density will linearly increase in relation to the number of transmitters.

B. UAV TRAJECTORY DETERMINATION

Three scheduled flight tests have been carried out to evaluate the performance of the prototype. The flight tests have been conducted on a route mapped out by 11 waypoints in an area close to the Tafira Campus of the University of Las Palmas de Gran Canaria. With the aim of facilitating explanation, the loiter mode is activated, and the altitude has been set to 20 m in all cases. The speeds of each flight are 2, 4 and 8 knots. Both AIS data, transmitted every 30 seconds by the UAV payload (according to the class B AIS rates in Table 1), and telemetry data, transmitted each second by the 433 MHz telemetry module, have been received and stored.

The AIS data include the MAMSL (meters above mean sea level) parameter, which indicates the flight altitude of the UAV. This parameter is transmitted as an AIS type 18 message in the HDT field, as explained in section III. In addition, the AIS transceiver is programmed with MMSI identification number 111224515, assigned according to a license application to the Ministry of Public Works of the Government of Spain.

To obtain the AIS data, a portable KSN-55 PilotsTECH AIS receiver was used. This AIS receiver has a sensitivity of −117 dBm and an approximate autonomy time of 12 hours. Additionally, the AIS receiver includes a Wi-Fi access point for connection with other devices provided with Internet access (PCs, smartphones, tablets, etc.), allowing the representation of the AIS data over a map through software such as OpenCPN [53]. The layout of the UAV payload mounting and the AIS portable receiver is shown in Figure 9.

Figure 10 shows the UAV trajectory during the first flight test (considering a constant speed of 2 knots). The tridimensional trajectories generated by the AIS positions (every 30 seconds) and the 433 MHz telemetry module (every second) are presented at the top of Figure 10. These positions have been converted into a KML file, generated by a script, and represented using the GoogleEarth Pro software. At the bottom of the same figure, the bidimensional representation of the trajectories generated by the telemetry module and the straight segments extracted from the AIS positions are presented. To compare the AIS and telemetry module trajectories, an interpolation is generated with the same number of points in both trajectories.

In Figure 10 (lower right), the AIS position errors in meters, determined by the module calculating the difference between both trajectories, are presented. Additionally, this graphic includes the theoretical maximum error for the AIS in meters, ϵ_t, which corresponds to half of the distance that the UAV can travel in a round trip to the same point for a determined speed; that is, $\epsilon_t(m) = v(m/s) \cdot \frac{t(s)}{2} = 1.0289 \cdot \frac{30}{2} = 15.43\ m$. As shown in the previous equation, the theoretical maximum error depends only on the speed of the drone, and this speed is dependent on the AIS report rate. Hence, ϵ_t does not depend on the followed trajectory, and it will have the same value for any trajectory for any speed of the same drone. Considering the case illustrated in Figure 10, a maximum error of 4.63 m when 74.08 m has been traveled is obtained at a location close to WP2. The results for the rest of the UAV speeds during the test flight are included in Table 3.

TABLE 3. Comparison between AIS and 433 MHz telemetry trajectories for a speed of 2 knots.

UAV speed	Maximum error	Theoretical maximum error
2 knots	4.63 m	15.43 m
4 knots	29.61 m	30.87 m
8 knots	42.58 m	42.58 m

V. CONCLUSION

In this article, the feasibility of using the AIS as a novel method for identifying and monitoring an amateur UAV has been discussed and demonstrated. The density of AIS messages in areas far from the coast is quite low, which thus enables the use of the prototype in these areas without significantly affecting the AIS's tracking and monitoring capabilities in the maritime environment. The implemented prototype has an appropriate weight and dimensions for avoiding drastically influencing the UAV's energy consumption. Including the sending of the height parameter, the use of the AIS allows tridimensional representations of the trajectory of the UAV. The prototype allows the acquisition of telemetry data of an amateur drone in near-real time, and with completely free access because of the absence of encryption in the AIS system. Moreover, it operates on a global and standardized wireless network.

With the introduction of the VDES system, the proposed identification and monitoring method can be derived to a new channel of general purpose, such as ASMs (Application-Specific Messages) or the VDE (VHF Data Exchange) for terrestrial links, avoiding its use in the AIS channels that will be used in maritime security. For this reason, future research directions should be addressed to extend the number of transmitted parameters by the UAV for identification and monitoring.

ACKNOWLEDGMENT

The authors acknowledge the work carried out by Juan Domingo Santana Urbín for his enormous contribution during this research. The support and continued assessment by MarineTraffic is also acknowledged.

REFERENCES

[1] S. Hayat, E. Yanmaz, and R. Muzaffar, "Survey on unmanned aerial vehicle networks for civil applications: A communications viewpoint," *IEEE Commun. Surveys Tuts.*, vol. 18, no. 4, pp. 2624–2661, 4th Quart., 2016, doi: 10.1109/COMST.2016.2560343.

[2] H. Kim, L. Mokdad, and J. Ben-Othman, "Designing UAV surveillance frameworks for smart city and extensive ocean with differential perspectives," *IEEE Commun. Mag.*, vol. 56, no. 4, pp. 98–104, Apr. 2018, doi: 10.1109/MCOM.2018.1700444.

[3] C. M. Gevaert, J. Suomalainen, J. Tang, and L. Kooistra, "Generation of spectral–temporal response surfaces by combining multispectral satellite and hyperspectral UAV imagery for precision agriculture applications," *IEEE J. Sel. Topics Appl. Earth Observ. Remote Sens.*, vol. 8, no. 6, pp. 3140–3146, Jun. 2015, doi: 10.1109/JSTARS.2015.2406339.

[4] P. Blank, S. Kirrane, and S. Spiekermann, "Privacy-aware restricted areas for unmanned aerial systems," *IEEE Secur. Privacy*, vol. 16, no. 2, pp. 70–79, Mar. 2018, doi: 10.1109/MSP.2018.1870868.

[5] R. L. Finn and D. Wright, "Unmanned aircraft systems: Surveillance, ethics and privacy in civil applications," *Comput. Law Secur. Rev.*, vol. 28, no. 2, pp. 184–194, Apr. 2012, doi: 10.1016/j.clsr.2012.01.005.

[6] C. Stöcker, R. Bennett, F. Nex, M. Gerke, and J. Zevenbergen, "Review of the current state of UAV regulations," *Remote Sens.*, vol. 9, no. 5, p. 459, May 2017, doi: 10.3390/rs9050459.

[7] Z. Kaleem, M. H. Rehmani, E. Ahmed, A. Jamalipour, J. J. P. C. Rodrigues, H. Moustafa, and W. Guibene, "Amateur drone surveillance: Applications, architectures, enabling technologies, and public safety issues: Part 1," *IEEE Commun. Mag.*, vol. 56, no. 1, pp. 14–15, Jan. 2018, doi: 10.1109/MCOM.2018.8255731.

[8] Z. Kaleem, M. H. Rehmani, E. Ahmed, A. Jamalipour, J. J. Rodrigues, H. Moustafa, and W. Guibene, "Amateur drone surveillance: Applications, architectures, enabling technologies, and public safety issues: Part 2," *IEEE Commun. Mag.*, vol. 56, no. 4, pp. 66–67, Apr. 2018, doi: 10.1109/MCOM.2018.8337898.

[9] G. Ding, Q. Wu, L. Zhang, Y. Lin, T. A. Tsiftsis, and Y.-D. Yao, "An amateur drone surveillance system based on the cognitive Internet of Things," *IEEE Commun. Mag.*, vol. 56, no. 1, pp. 29–35, Jan. 2018, doi: 10.1109/MCOM.2017.1700452.

[10] I. Guvenc, F. Koohifar, S. Singh, M. L. Sichitiu, and D. Matolak, "Detection, tracking, and interdiction for amateur drones," *IEEE Commun. Mag.*, vol. 56, no. 4, pp. 75–81, Apr. 2018, doi: 10.1109/MCOM.2018.1700455.

[11] M. Z. Anwar, Z. Kaleem, and A. Jamalipour, "Machine learning inspired sound-based amateur drone detection for public safety applications," *IEEE Trans. Veh. Technol.*, vol. 68, no. 3, pp. 2526–2534, Mar. 2019, doi: 10.1109/TVT.2019.2893615.

[12] X. Yue, Y. Liu, J. Wang, H. Song, and H. Cao, "Software defined radio and wireless acoustic networking for amateur drone surveillance," *IEEE Commun. Mag.*, vol. 56, no. 4, pp. 90–97, Apr. 2018, doi: 10.1109/MCOM.2018.1700423.

[13] X. Chang, C. Yang, J. Wu, X. Shi, and Z. Shi, "A surveillance system for drone localization and tracking using acoustic arrays," in *Proc. IEEE 10th Sensor Array Multichannel Signal Process. Workshop (SAM)*, Jul. 2018, pp. 573–577, doi: 10.1109/SAM.2018.8448409.

[14] A. Schumann, L. Sommer, T. Müller, and S. Voth, "An image processing pipeline for long range UAV detection," *Proc. SPIE*, vol. 10799, Oct. 2018, Art. no. 107990T, doi: 10.1117/12.2325735.

[15] T. Müller, "Robust drone detection for day/night counter-UAV with static VIS and SWIR cameras," *Proc. SPIE*, vol. 10190, May 2017, Art. no. 1019018, doi: 10.1117/12.2262575.

[16] F. Hoffmann, M. Ritchie, F. Fioranelli, A. Charlish, and H. Griffiths, "Micro-Doppler based detection and tracking of UAVs with multistatic radar," in *Proc. IEEE Radar Conf. (RadarConf)*, May 2016, pp. 1–6, doi: 10.1109/RADAR.2016.7485236.

[17] N. Mohajerin, J. Histon, R. Dizaji, and S. L. Waslander, "Feature extraction and radar track classification for detecting UAVs in civillian airspace," in *Proc. IEEE Radar Conf.*, May 2014, pp. 674–679, doi: 10.1109/RADAR.2014.6875676.

[18] I. Bisio, C. Garibotto, F. Lavagetto, A. Sciarrone, and S. Zappatore, "Unauthorized amateur UAV detection based on WiFi statistical fingerprint analysis," *IEEE Commun. Mag.*, vol. 56, no. 4, pp. 106–111, Apr. 2018, doi: 10.1109/MCOM.2018.1700340.

[19] M. M. Azari, H. Sallouha, A. Chiumento, S. Rajendran, E. Vinogradov, and S. Pollin, "Key technologies and system trade-offs for detection and localization of amateur drones," *IEEE Commun. Mag.*, vol. 56, no. 1, pp. 51–57, Jan. 2018, doi: 10.1109/MCOM.2017.1700442.

[20] M. Fujii, K. Yamashita, M. Urakami, and N. Wakabayashi, "The study of simple navigation system for small craft using class B AIS," in *Proc. OCEANS*, Apr. 2014, pp. 1–4, doi: 10.1109/OCEANS-TAIPEI.2014.6964411.

[21] R. J. Wallace, K. M. Kiernan, J. Robbins, and T. Haritos, "Small unmanned aircraft system operator compliance with visual line of sight requirements," *Int. J. Aviation, Aeronaut., Aerosp.*, vol. 6, no. 2, p. 3, 2019, doi: 10.15394/ijaaa.2019.1327.

[22] *CRFS*. Accessed: Dec. 25, 2019. [Online]. Available: https://www.crfs.com/drone-detection/

[23] M. Guterres, S. Jones, G. Orrell, and R. Strain, "ADS-B surveillance system performance with small UAS at low altitudes," in *Proc. AIAA Inf. Syst.-AIAA Infotech Aerosp.*, Jan. 2017, p. 1154, doi: 10.2514/6.2017-1154.

[24] L. R. Sahawneh, M. O. Duffield, R. W. Beard, and T. W. McLain, "Detect and avoid for small unmanned aircraft systems using ADS-B," *Air Traffic Control Quart.*, vol. 23, nos. 2–3, pp. 203–240, Apr. 2015, doi: 10.2514/atcq.23.2-3.203.

[25] M. Leonardi and E. Giuseppe Piracci, "ADS-B degarbling and jamming mitigation by the use of blind source separation," in *Proc. IEEE/AIAA 37th Digit. Avionics Syst. Conf. (DASC)*, Sep. 2018, pp. 1–5, doi: 10.1109/DASC.2018.8569598.

[26] D. Green, C. Fowler, D. Power, and J. K. E. Tunaley, "VHF propagation study," Defence R&D Canada, Toronto, ON, Canada, Contract Rep. R-11-020-868, Sep. 2011.

[27] S. Plass, R. Poehlmann, R. Hermenier, and A. Dammann, "Global maritime surveillance by airliner-based AIS detection: Preliminary analysis," *J. Navigat.*, vol. 68, no. 6, pp. 1195–1209, Nov. 2015, doi: 10.1017/S0373463315000314.

[28] *Maritime Navigation and Radiocommunication Equipment and Systems—Class B Shipborne Equipment of the Automatic Identification System (AIS)—Part 1: Carrier-Sense Time Division Multiple Access (CSTDMA) Techniques*, Standard IEC 62287-1, IEC, 2006, doi: 10.31030/2760941 .

[29] S.-J. Chang, C.-H. Huang, G. Hsu, and S.-M. Chang, "Implementation of AIS-based marine meteorological applications," in *Proc. OCEANS*, Apr. 2014, pp. 1–4, doi: 10.1109/OCEANS-TAIPEI.2014.6964499.

[30] D. Inazu, T. Ikeya, T. Waseda, T. Hibiya, and Y. Shigihara, "Measuring offshore tsunami currents using ship navigation records," *Progr. Earth Planet. Sci.*, vol. 5, no. 1, p. 38, 2012, doi: 10.1186/s40645-018-0194-5.

[31] T. K. Liu, H. Y. Sheu, and Y. T. Chen, "Utilization of vessel automatic identification system (AIS) to estimate the emission of air pollutant from merchant vessels in a port area," in *Proc. OCEANS*, 2015, pp. 1–5, doi: 10.1109/OCEANS-Genova.2015.7271680.

[32] M. Tichavska and B. Tovar, "Port-city exhaust emission model: An application to cruise and ferry operations in Las Palmas port," *Transp. Res. A, Policy Pract.*, vol. 78, pp. 347–360, Aug. 2015, doi: 10.1016/j.tra.2015.05.021.

[33] J. H. Song, K. R. Oh, I. K. Kim, and J. Y. Lee, "Application of maritime AIS (automatic identification system) to ADS-B (automatic dependent surveillance—broadcast) transceiver," in *Proc. ICCAS*, Oct. 2010, pp. 2233–2237. [Online]. Available: https://ieeexplore.ieee.org/document/5669842

[34] P. Lessing, L. Bernard, B. Tetreault, and J. Chaffin, "Use of the automatic identification system (AIS) on autonomous weather buoys for maritime domain awareness applications," in *Proc. OCEANS*, Sep. 2006, pp. 1–6, doi: 10.1109/OCEANS.2006.307023.

[35] F. Lázaro, R. Raulefs, W. Wang, F. Clazzer, and S. Plass, "VHF data exchange system (VDES): An enabling technology for maritime communications," *CEAS Space J.*, vol. 11, no. 1, pp. 55–63, Mar. 2019, doi: 10.1007/s12567-018-0214-8.

[36] T. Eriksen, G. Høye, B. Narheim, and B. J. Meland, "Maritime traffic monitoring using a space-based AIS receiver," *Acta Astronautica*, vol. 58, no. 10, pp. 537–549, May 2006, doi: 10.1016/j.actaastro.2005.12.016.

[37] V. F. Arguedas, G. Pallotta, and M. Vespe, "Maritime traffic networks: From historical positioning data to unsupervised maritime traffic monitoring," *IEEE Trans. Intell. Transp. Syst.*, vol. 19, no. 3, pp. 722–732, Mar. 2018, doi: 10.1109/TITS.2017.2699635.

[38] E. Alincourt, C. Ray, P.-M. Ricordel, D. Dare-Emzivat, and A. Boudraa, "Methodology for AIS signature identification through magnitude and temporal characterization," in *Proc. OCEANS*, Apr. 2016, pp. 1–6, doi: 10.1109/OCEANSAP.2016.7485420.

[39] *Standard for Interfacing Marine Electronic Devices*, Standard NMEA 0183, NMEA, 2002.

[40] A. Koubâa, A. Allouch, M. Alajlan, Y. Javed, A. Belghith, and M. Khalgui, "Micro air vehicle link (MAVLink) in a nutshell: A survey," *IEEE Access*, vol. 7, pp. 87658–87680, 2019, doi: 10.1109/ACCESS.2019.2924410.

[41] S. Atoev, K. Kwon, S. Lee, and K. Moon, "Data analysis of the MAVLink communication protocol," in *Proc. Int. Conf. Inf. Sci. Commun. Technol. (ICISCT)*, Tashkent, Uzbekistan, Nov. 2017, pp. 1–3, doi: 10.1109/ICISCT.2017.8188563.

[42] *eCalc*. Accessed: Dec. 25, 2019. [Online]. Available: https://www.ecalc.ch

[43] *3D Robotics. Y6 Model*. Accessed: Jan. 10, 2020. [Online]. Available: https://3dr.com/support/articles/3dr_y6_conversion_kit/
[44] *Pixhawk*. Accessed: Jan. 10, 2020. [Online]. Available: https://pixhawk.org/
[45] *Raspberry Pi 3 Model B*. Accessed: Jan. 10, 2020. [Online]. Available: https://www.raspberrypi.org/products/raspberry-pi-3-model-b/
[46] E. Husni and N. Febrian, "Thermal validation testing of an automatic identification system (AIS) receiver for low earth orbit (LEO) CubeSat," *J. Phys., Conf. Ser.*, vol. 1152, Jan. 2019, Art. no. 012006, doi: 10.1088/1742-6596/1152/1/012006.
[47] R. G. V. Meyer, W. Kleynhans, and D. Swanepoel, "Smarter than your average sensor: AIS sensor that intelligently re-transmits meaningful information derived from RawAIS in network limited areas," in *Proc. Int. Arch. Photogramm., Remote Sens. Spatial Inf. Sci.*, 2017, p. 113, doi: 10.5194/isprs-archives-XLII-3-W2-113-2017.
[48] *SRT Marine Systems PLC*. Accessed: Jan. 10, 2020. [Online]. Available: https://srt-marine.com/product/ais-transceiver-modules/
[49] *Technical Characteristics for an Automatic Identification System Using Time-Division Multiple Access in the VHF Maritime Mobile Band*, document ITU-R M.1371-5, International Telecommunications Union, 2014.
[50] MarineTraffic. *Ship Tracking Intelligence*. Accessed: Nov. 14, 2018. [Online]. Available: http://www.marinetraffic.com
[51] M. Tichavska, F. Cabrera, B. Tovar, and V. Araña, "Use of the automatic identification system in academic research," in *Proc. Int. Conf. Comput. Aided Syst. Theory*. Cham, Switzerland: Springer, Feb. 2015, pp. 33–40, doi: 10.1007/978-3-319-27340-2_5.
[52] F. Cabrera, N. Molina, M. Tichavska, and V. Araña, "Automatic identification system modular receiver for academic purposes," *Radio Sci.*, vol. 51, no. 7, pp. 1038–1047, Jul. 2016, doi: 10.1002/2015RS005895.
[53] *OpenCPN*. Accessed: Dec. 25, 2019. [Online]. Available: https://www.opencpn.org

NICOLÁS MOLINA-PADRÓN was born in Gáldar, Las Palmas, Spain, in 1991. He received the bachelor's degree in technologies for telecommunications engineering and the master's degree in telecommunications engineering from the University of Las Palmas de Gran Canaria, Spain, in 2015 and 2017, respectively. He is currently working on his Ph.D. thesis about signal processing techniques applied to software defined radio (SDR) devices.

He has been working as a Research Assistant with Institute for Technological Development and Innovation in Communications (IDeTIC), since 2015. His activities have been related to communication systems prototyping for drone and maritime applications.

FRANCISCO CABRERA-ALMEIDA (Member, IEEE) was born in Las Palmas de Gran Canaria, Spain, in 1970. He received the degree in telecommunications engineering from the Universidad de Las Palmas de Gran Canaria (ULPGC), Spain, in 1997, and the Ph.D. degree from ULPGC, in 2012. He is currently an Assistant Professor with the Signal and Communications Department, ULPGC. He has participated in a number of Spanish and European projects in collaboration with industries and other universities. His research interests include numerical electromagnetic modeling techniques, radio wave propagation, and communications systems applied to data acquisition complex networks.

VÍCTOR ARAÑA (Member, IEEE) was born in Las Palmas de Gran Canaria, Spain, in 1965. He received the degree in telecommunication engineering from the Universidad Politécnica de Madrid, Madrid, Spain, in 1990, and the Ph.D. degree from the Universidad de Las Palmas de Gran Canaria (ULPGC), Las Palmas, Spain, in 2004. He is currently an Assistant Professor with the Signal and Communication Department, ULPGC. He has been the leading researcher in several Spanish research and development projects. He has taken part in a number of Spanish and European projects in collaboration with industries. His research interests include the nonlinear design of microwave circuits, control subsystem units, and communications systems applied to data acquisition complex networks.

MILUŠE TICHAVSKA received the degree from the Department of Applied Economics, Universidad de Las Palmas de Gran Canaria (ULPGC). She is a University Industry Relations professional with a broad scientific background on a Ph.D. level. Throughout her years as a Research Fellow, she specialized in AIS-based vessel emission calculations, externality costs and eco-efficiency in ports. Her work has been published in international peer-reviewed journals and presented at international conferences. Her research interests include the fields of telecommunications, and applied economics and applications in operations management, especially in supply chain management. She has received scholarships awarded by ULPGC as a reward for excellence in her academic and professional trajectory, including a Fellowship for her Ph.D. studies. Moreover, she has participated in various Spanish and EU funded research projects. She received the Extraordinary Doctorate Award, in 2017, based on the design, quality, and originality of her published research, among other academic merits.

BLAS-PABLO DORTA-NARANJO was born in Las Palmas, Spain, in 1957. He received the M.Sc. degree in electrical engineering and the Ph.D. degree from the Technical University of Madrid (UPM), Spain, in 1983 and 1991, respectively.

He joined the Grupo de Microondas y Radar, Departamento de Señales, Sistemas y Radiocomunicaciones, UPM, where he was an Associate Professor, until 1998. Since 1998, he has been a Full Professor with the Departamento de Señales y Communicaciones, Universidad de Las Palmas de Gran Canaria, Spain. His research activities include the area of design of high-frequency circuits and subsystems, such as synthesizers and PLLs, oscillators, multipliers, and frequency dividers for communications and radar systems in hybrid and MMIC technologies.